space vector modulated Hybrid Series Active Filter for Harmonic Compensation

Sushree Diptimayee Swain*, Pravat Kumar Ray† and Kanungo Barada Mohanty‡
Department of Electrical Engineering
National Institute of Technology, Rourkela, Rourkela-769 008, India
*sushreedipti@gmail.com †rayp@nitrkl.ac.in ‡kbmohanty@nitrkl.ac.in

Abstract—This paper deals with the implementation of Hybrid Series Active Power Filter (HSAPF) for compensation of harmonic voltage and current using Space Vector Pulse Width Modulation (SVPWM) technique. The Hybrid control approach based Synchronous Reference Frame(SRF) method is used to generate the appropriate reference voltages for HSAPF to compensate reactive power. This HSAPF uses PI control to the outer DC-link voltage control loop and SVPWM to the inner voltage control loop. The switching pattern for the switching of the inverter of series active power filter in HSAPF is generated using SVPWM technique. The proposed HSAPF is verified through MATLAB Simulink version R2010 for SRF control strategy and SVPWM technique. The simulated results verified that for both SRF-SVPWM based HSAPF and Synchronous Reference Frame with Carrier Based Pulse Width Modulation (SRF-CBPWM) based HSAPF shows that the Total Harmonic Distortion (THD) of source current for steady state as well as dynamic condition of non-linear load follows the IEEE Std.519-1992.

Index Terms—Hybrid series active power filter, harmonic producing non-linear load, Carrier Based Pulse Width Modulation(CBPWM), Space Vector Pulse Width Modulation.

I. Introduction

In recent years, huge usage of power electronic devices such as thyristors, diodes, rectifiers, lighting equipments, uninterruptible power supplies (UPS), arc furnaces etc. creates large scale of harmonics in power systems. These harmonics cause many unwanted effects on Power Quality (PQ) such as undesirable computer network failures, premature motor burnouts, humming in telecommunication lines, excessive heating in rotating machines, interference with communication circuits, harmonics resonances in the utility and transformer overheating etc. are few examples of poor power quality in power system. Traditionally Passive Power Filters (PPFs) [1], [2], [3] are used to reduce harmonics, but PPFs are unable to filter out the harmonics in transient condition. The major drawbacks of PPFs are heavy in weight, large in size, bulky, fixed compensation and resonance phenomena. Recently, some Active Power Filters [4], [5], [6], [7], [8] are widely used for the compensation of harmonics in power systems. The function of active power filter is, to inject harmonic current or voltage into the power system with magnitudes same as the harmonic current or voltage produced by a nonlinear load, but with $180\,\mathrm{deg}$ phase shift. These APFs are require a controlled voltage source inverter for producing a reference compensating voltage or current. Active Power Filters (APFs) [2] are capable of damping out the harmonic resonance phenomenon between the PPFs and source impedance. But the usage of only APFs is a very costly solution because it needs comparatively very large power converter ratings. Considering the merits of PPFs and APFs, Hybrid Active Power Filters are designed HAPFs [9], [10] are very much efficient for reactive power and harmonic compensation. The design of HAPFs are based on cutting-edge power electronics technology, which includes power conversion circuits, semiconductor devices, analog/digital signal processing, voltage/current sensors and control theory. In active and hybrid power filters, a number of control strategies such as Hysteresis [11], [12], sliding mode control techniques [13], [14] carrier based control [15] techniques are used to regulate the current and voltage generated by the voltage source inverter. But in all the previous cases frequency is variable. Hence, there may be difficulty in the design as well as in the control of noise level. PWM control technique can eliminate these problems. Earlier numerous Pulse Width Modulation (PWM) techniques have already been investigated, among them SVPWM [16], [17] is most dynamic and energetic because of its reliability, robustness, simplicity both in hardware and software and also its performance is awesome with small modulation ratio. But the SVPWM is very critical when the no. of levels of PWMVSI increases and also it is very complicated in some steps of switching pattern generation. SVPWM depends on CBPWM (carrier based PWM) for achieving better performance. The objective of this paper is to investigate the detailed study of SVPWM, the difference between SRF-SVPWM and SRF-CBPWM.In order to obtain a better control and better performance, a simple and efficient control scheme is required. That's why SRF-CBPWM and SRF-SVPWM both used as control algorithm for reference generation process. The $\alpha - \beta$ transformation is applied to the control scheme design and aims to generate the reference voltage directly in $\alpha - \beta$ reference frame.

The paper is organised as follows, the circuit topology for three phase HSAPF is described in section-II, section-III depicts the control algorithm for Series Active part of hybrid filter, section-IV disclose the controller design for HSAPF using SVPWM, section-V explains the simulation results for harmonic compensation using HSAPF. Section-VI concludes the paper.
[1]

[1]978-1-4673-6540-6/15/$31.00 2015 IEEE

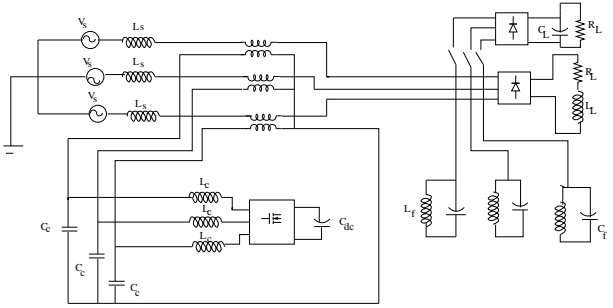

Fig. 1. Hybrid series active filter with 2 types of nonlinear loads

II. Circuit topology for three phase Hybrid Series Active Power filter (HSAPF)

The circuit diagram includes a series active filter and shunt connected passive power filter[1]. The active filter is connected in series with the source and non-linear load through a matching transformer of turn ratio $1:1$ and the passive power filter is connected in parallel with the non-linear load. The PPF includes a third order, fifth order tuned harmonic filters for the harmonic compensation of current on load side. One converter is connected in series in each phase through a matching transformer with a turn ratio equal to $1:1$. This transformer is required for isolation purposes. The DC side capacitor is common for all three converters. A PWM control block is designed so that the AC output voltage of the converters follows the references that are calculated by the control block based on the hybrid control approach based synchronous reference frame method.

III. Synchronous Reference Frame Method for Active Filter Design

In this method three phase measured load voltages are transformed from stationary reference frame to rotating reference frame with fundamental frequency as:

$$\begin{bmatrix} V_d \\ V_q \end{bmatrix} = \frac{2}{3}\begin{bmatrix} \cos\theta & \cos(\theta-\frac{2\pi}{3}) & \cos(\theta+\frac{2\pi}{3}) \\ \sin\theta & \sin(\theta-\frac{2\pi}{3}) & \sin(\theta+\frac{2\pi}{3}) \end{bmatrix}\begin{bmatrix} V_{La} \\ V_{Lb} \\ V_{Lc} \end{bmatrix} \quad (1)$$

A Phase Locked Loop (PLL) tracks the phase angle of the source voltage, which is necessary for transformation. The obtained voltages can be divided into average and oscillating components.

$$V_d = \overline{V_d} + \tilde{V_d} \quad (2)$$

$$V_q = \overline{V_q} + \tilde{V_q} \quad (3)$$

Where , V_{La}, V_{Lb}, V_{Lc} , are load voltages, which are distorted or asymmetrical in nature. If the dq-components are Low Pass Filtered (LPF) and this LPFs output is subtracted from original, the DC-components are eliminated and one can get the total harmonic contents.

$$\tilde{V_d} = V_d - \overline{V_d} \quad (4)$$

$$\tilde{V_q} = V_q - \overline{V_q} \quad (5)$$

By inverse transformation one can obtain the distorted or harmonic components of the load voltages after the compensation of shunt passive power filter.

$$\begin{bmatrix} V_{Lah} \\ V_{Lbh} \\ V_{Lch} \end{bmatrix} = \begin{bmatrix} \cos\theta & \sin\theta \\ \cos(\theta-\frac{2\pi}{3}) & \sin(\theta-\frac{2\pi}{3}) \\ \cos(\theta+\frac{2\pi}{3}) & \sin(\theta+\frac{2\pi}{3}) \end{bmatrix}\begin{bmatrix} \tilde{V_d} \\ \tilde{V_q} \end{bmatrix} \quad (6)$$

Therefore, the three phase source currents ,I_{sa}, I_{sb}, I_{sc} , are transformed into rotating reference frame as:

$$\begin{bmatrix} I_d \\ I_q \end{bmatrix} = \frac{2}{3}\begin{bmatrix} \cos\theta & \cos(\theta-\frac{2\pi}{3}) & \cos(\theta+\frac{2\pi}{3}) \\ \sin\theta & \sin(\theta-\frac{2\pi}{3}) & \sin(\theta+\frac{2\pi}{3}) \end{bmatrix}\begin{bmatrix} I_{sa} \\ I_{sb} \\ I_{sc} \end{bmatrix} \quad (7)$$

The obtained currents I_d and I_q have both DC and AC components.

$$I_d = \overline{I_d} + \tilde{I_d} \quad (8)$$

$$I_q = \overline{I_q} + \tilde{I_q} \quad (9)$$

If the dq-components of current are low pass filtered and again subtracted from the original components, one can obtains the total harmonic content and the DC-components are eliminated. Using inverse transformation, harmonic components of source current can be obtained as :

$$\begin{bmatrix} I_{sah} \\ I_{sbh} \\ I_{sch} \end{bmatrix} = \begin{bmatrix} \cos\theta & \sin\theta \\ \cos(\theta-\frac{2\pi}{3}) & \sin(\theta-\frac{2\pi}{3}) \\ \cos(\theta+\frac{2\pi}{3}) & \sin(\theta+\frac{2\pi}{3}) \end{bmatrix}\begin{bmatrix} \tilde{I_d} \\ \tilde{I_q} \end{bmatrix} \quad (10)$$

The generation of reference compensating signal using the combined load voltage and source current detection scheme is shown in Fig. 2. From fig.2, the error between the reference and the actual DC-link voltage of DC-link capacitor of three phase PWM inverter fed from the ac system is first passed through a PI controller and then it is subtracted from the oscillatory component in d-axis. Since the extra fundamental components are added to harmonic components respectively. Thus the reference compensating voltages are also expressed as:

$$\left.\begin{aligned} V_{ca}^{*} &= K I_{sah} - V_{Lah} + \Delta V_{caf} \\ V_{cb}^{*} &= K I_{sbh} - V_{Lbh} + \Delta V_{cbf} \\ V_{cc}^{*} &= K I_{sch} - V_{Lbh} + \Delta V_{ccf} \end{aligned}\right\} \quad (11)$$

IV. Controller design for HSAPF using SVPWM technique

The Space Vector Pulse Width Modulation (SVPWM) is generally used as voltage controller to control the IGBT switches of HSAPF. It consists of six IGBT switches (s1-s6). Depending upon different switching combination, PWMVSI produce different outputs. This SVPWM is different from other PWM methods, because it produces a vector as a reference so SVPWM is better than other PWM methods. Reference vector is nothing but the reference compensating voltage generated by SRF method in $\alpha\beta$-plane. The ON-OFF position of switch is based on the presence of reference voltage vector on $\alpha\beta$-plane. The switches 1,3,5 are the upper switches and switches 2,4,6 are lower switches of PWMVSI. Switches are ON means '1' and switches are OFF means '0'. If all

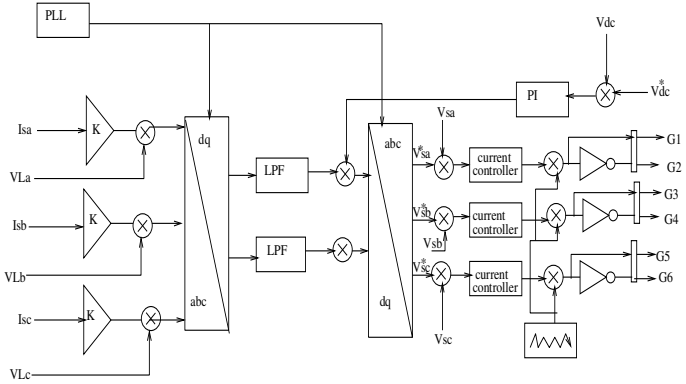

Fig. 2. Block diagram for reference compensator voltage generation by SRF technique and switching pattern generation by CBPWM

upper switches are ON, then upper inverter leg ON and the terminal voltage is +ve. If all the upper switches are OFF i.e. zero, so the terminal voltage is zero.

The upper switches are reciprocal of lower switches. So

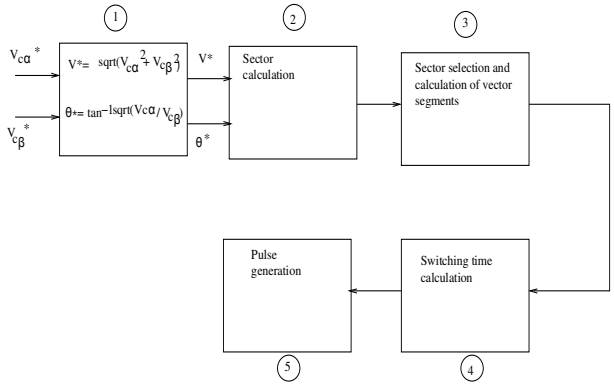

Fig. 3. (a)Block diagram for SVPWM implementation

the probable association of switching states are: 000, 001, 010, 011, 100, 101, 110, 111. There are '8' switching states, among them six active switching states (v1-v6) and two zero switching states(V0). The zero vectors are placed in the origin of axis. Control procedure of SVPWM consists of 4-steps as follows Step-1: calculation of magnitude and angle of the reference voltage vector Step-2: Determination of sector and switching time duration TA, TB, TC for each sector. Step-3: calculation of duty time for both upper and lower switches. Step-4: comparision of duty time with the triangular carrier to generate 6-pulses for IGBTs. Control procedure for SVPWM technique are shown in Fig.3. Step-1: Calculation of magnitude and angle of the reference voltage vector are given below

$$|V^*| = \sqrt{V_{c\alpha}^{*2} + V_{c\beta}^{*2}} \tag{12}$$

$$\theta^* = \tan^{-1}\left(\frac{V_{c\beta}^*}{V_{c\alpha}^*}\right) \tag{13}$$

Where $V^*_{c\alpha}$ and $V^*_{c\beta}$ are the reference compensating voltage produced by SRF method in $\alpha\beta$-plane, V^* is the reference voltage vector, θ^* is the reference angle. Step-2: Sector defines, in which sector the reference output takes rest, for that the calculation of switching time and switching sequence is required. Time duration: V^* build up with two active and one zero vector. For sector1 (0 to pi/3): V^* can be construct with V_0 , V_1 , and V_2. V^* can be calculated in terms of duration time as

$$V_{ref}.T_c = V_1.T_1/T_2 + V_2.T_2/T_c + V_0.T_0/T_c \tag{14}$$

$$V^* = V_1T_1 + V_2T_2 + V_0T_0 \tag{15}$$

T_c is the total cycle

$$T_c = T_1 + T_2 + T_0 \tag{16}$$

The location of V^*, V_1, V_2, V_0 is explained in terms of magnitude and angle as follows:

$$V^* = V^* r^{j\theta} \tag{17}$$

$$V_1 = \frac{2}{3}V_{dc} \tag{18}$$

$$V_2 = \frac{2}{3}V_{dc}e^{j\frac{\pi}{3}} \tag{19}$$

$$V_0 = 0 \tag{20}$$

$$r^{j\theta} = \cos\theta + j\sin\theta \tag{21}$$

$$e^{j\frac{\pi}{3}} = \cos\frac{\pi}{3} + j\sin\frac{\pi}{3} \tag{22}$$

Put the values of $V^*, V_1, V_2 \& V_0$ in (23)

$$T_c * V^* * \begin{bmatrix}\cos\theta\\ \sin\theta\end{bmatrix} = T_1 * \frac{2}{3}V_{dc}\begin{bmatrix}1\\ 0\end{bmatrix} + T_2 * \frac{2}{3}V_{dc}\begin{bmatrix}\cos\frac{\pi}{3}\\ \sin\frac{\pi}{3}\end{bmatrix} \tag{23}$$

Separating the real and imaginary terms in (23), $T_1 and T_2$ can be calculated as

$$T_1 = T_c * \frac{\sqrt{3}V^*}{Vdc}\sin\left(\frac{\pi}{3} - \theta\right) = T_c * a * \sin\left(\frac{\pi}{3} - \theta\right) \tag{24}$$

$$T_2 = T_c * a * \sin\theta, \tag{25}$$

$$0 < \theta < \frac{\pi}{3} \tag{26}$$

'a' is the modulation index. The general calculation of duty times for 'n' no. of sectors as,

$$T_1 = T_c * a * \sin\left(\frac{\pi}{3} - \theta + \frac{n-1}{3} * \pi\right) \quad (27)$$

$$T_1 = T_c * a \left[\sin\left(\frac{n\pi}{3}\right) * \cos\theta - \cos\left(\frac{n\pi}{3}\right) * \sin\theta\right] \quad (28)$$

$$T_2 = T_c * a \left[-\cos\theta * \sin\left(\frac{(n-1)\pi}{3}\right) + \sin\theta * \cos\left(\frac{(n-1)\pi}{3}\right)\right] \quad (29)$$

$$T_0 = T_c - T_1 - T_2 \quad (30)$$

Step-3: Duty time calculation for each sector Each sector consists of 7 switching states for each cycle i.e. sector-1 passes through these switching states:000-100-110-111-110-100-000, one round and again return back. This occurs at time Tc and it is divisible among the 7 switching states. Three of them are zero vectors.

$$T_c = \frac{T_0}{4} + \frac{T_1}{2} + \frac{T_0}{2} + \frac{T_2}{2} + \frac{T_1}{2} + \frac{T_0}{4} \quad (31)$$

For sector-1, the switch is ON between $T_0 \& T_c - \frac{T_0}{4}$ in the first phase, between $\frac{T_0}{4} + \frac{T_1}{2}$ and for second phase, and so on. The duty time for each sector is shown in Table-1. Step-4: Comparision of T_1, T_2, T_0 with the triangular carrier to generate 6-pulses for IGBT switches.

Table.1

sector	upper switches: S1, S3, S5	Lower switches: S4, S6, S2
1	$S1 = T_A + T_B + \frac{T_0}{2}$ $S3 = T_B + \frac{T_0}{2}$ $S5 = \frac{T_0}{2}$	$S4 = \frac{T_0}{2}$ $S6 = T_A + \frac{T_0}{2}$ $S2 = T_A + T_B + \frac{T_0}{2}$
2	$S1 = T_A + \frac{T_0}{2}$ $S3 = T_A + T_B + \frac{T_0}{2}$ $S5 = \frac{T_0}{2}$	$S4 = T_B + \frac{T_0}{2}$ $S6 = \frac{T_0}{2}$ $S2 = T_A + T_B + \frac{T_0}{2}$
3	$S1 = \frac{T_0}{2}$ $S3 = T_A + T_B + \frac{T_0}{2}$ $S5 = T_B + \frac{T_0}{2}$	$S4 = T_A + T_B + \frac{T_0}{2}$ $S6 = \frac{T_0}{2}$ $S2 = T_A + \frac{T_0}{2}$
4	$S1 = T_B + \frac{T_0}{2}$ $S3 = T_A + \frac{T_0}{2}$ $S5 = T_A + T_B + \frac{T_0}{2}$	$S4 = T_A + \frac{T_0}{2}$ $S6 = T_B + \frac{T_0}{2}$ $S2 = \frac{T_0}{2}$
5	$S1 = T_A + T_B + \frac{T_0}{2}$ $S3 = \frac{T_0}{2}$ $S5 = T_A + T_B + \frac{T_0}{2}$	$S4 = \frac{T_0}{2}$ $S6 = T_A + T_B + \frac{T_0}{2}$ $S2 = \frac{T_0}{2}$
6	$S1 = \frac{T_0}{2}$ $S3 = \frac{T_0}{2}$ $S5 = T_A + \frac{T_0}{2}$	$S4 = T_A + T_B + \frac{T_0}{2}$ $S6 = T_B + \frac{T_0}{2}$ $S2 = \frac{T_0}{2}$

V. Passive Power Filter

The Passive Power Filter(PPF) is connected in parallel with the load. The PPF includes the parallel combination of L and C components. The PPF presents high impedance at fundamental frequency and offers very less impedance at all harmonic frequencies. PPF provide less impedance for harmonic current to prevent their flow towards source side.
L_f andC_f -Are the PPF inductances and PPF capacitances Z_{spf} is the PPF impedance The PPF impedance given as

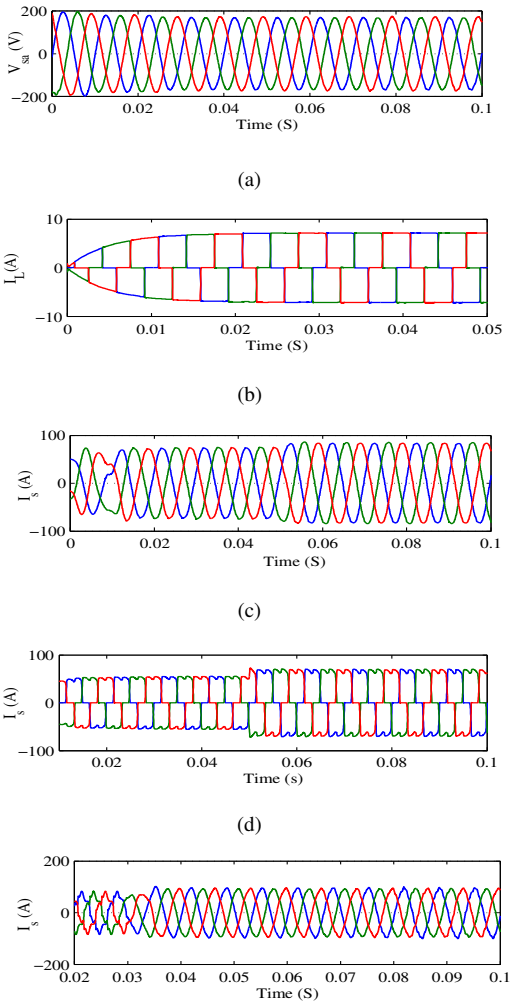

Fig. 4. (a)Source voltage, Steady state response of (b) load current (c) source current, Transient response of (d)load current (e) source current for SRF-CBPWM based HSAPF

follows

$$Z_{spf} = \frac{sL_f}{s^2 L_f C_f + 1} \quad (32)$$

$$Z_{spf} = \frac{J w L_f}{1 - L_f C_f w^2} \quad (33)$$

when

$$w << \frac{1}{L_f C_f} Z_{spf} = wL_f \quad (34)$$

i.e The filters impedance is inductive for lower frequencies when

$$w >> \frac{1}{L_f C_f} \quad (35)$$

$$\Rightarrow Z_{spf} = \frac{1}{C_f w} \quad (36)$$

The filters impedance is capacitive for all harmonics. F_r is the resonant frequency

$$F_r = \frac{1}{2\pi} \sqrt{\frac{1}{L_f C_f}} \quad (37)$$

VI. Simulation Results for Harmonic Compensation using HSAPF

The performance of HSAPF has been tested through MATLAB/Simulink. Since the simulations are carried out in a PC having MS windows 32-bit version installed with MATLAB R2010a. A 3-phase ideal supply voltage is applied to a harmonic voltage producing non-linear load. This voltage producing non-linear load consists of a 3-phase diode bridge rectifier feeding an RL-load. These are two non-linear loads taken here are: Load-1 consists of 3-phase diode bridge rectifier with a series RL-load connected at DC side, load-2: consists of 3-phase diode bridge rectifier with variable resistor. Due to this type of non-linear load a harmonic distortion occurs in source current. This harmonic pollution causes power quality disturbances. So power quality disturbances can be eliminated by means of HSAPF. Table-I summarizes the simulation parameters. Where Ls and Rs are known as source inductance and source resistance. Lf and Rf are known as filter inductance and resistance, Vs is supply mains voltage, C is the DC-link capacitance, Kp and Ki are the PI controller gains, f is the system frequency, Lpf, Cpf are the passive filter inductance and capacitance. One control approach and two modulation techniques i.e. SRF-CBPWM and SRF-SVPWM are verified and analysed using the following MATLAB simulation results. At the beginning for steady state condition, only load-1 is taken into operation untill t=0.3s, and then measured the harmonics compensation ability of HSAPF. The performance of HSAPF is accessed under dynamic condition has been noticed by sudden change on load i.e. load-2 within t=0.02s to t=0.1s for current harmonic compensation. In order to investigate the validity of the proposed controller, the system is simulated under MATLAB/simulink version 2010. The goal of simulation is to compare the result of SRF-SVPWM based HSAPF with SRF-CBPWM based HSAPF. The THD response of SRF-SVPWM based HSAPF is very less in comparision to THD of HSAPF with SRF-CBPWM. Also SRF-SVPWM utilizes dc-link voltage properly for switching pattern generation but SRF-CBPWM can not use dc-link voltage for PWM generation. Simulated waveforms for supply voltage(Vs), load current(IL), source current(Is),dc-link voltage for both steady state as well as transient condition are presented in Fig. 4 and in Fig. 5 respectively. The nature of source current without filter is exactly like load current. FFT analysis has been carried out for HSAPF(i.e. for both SRF-SVPWM and

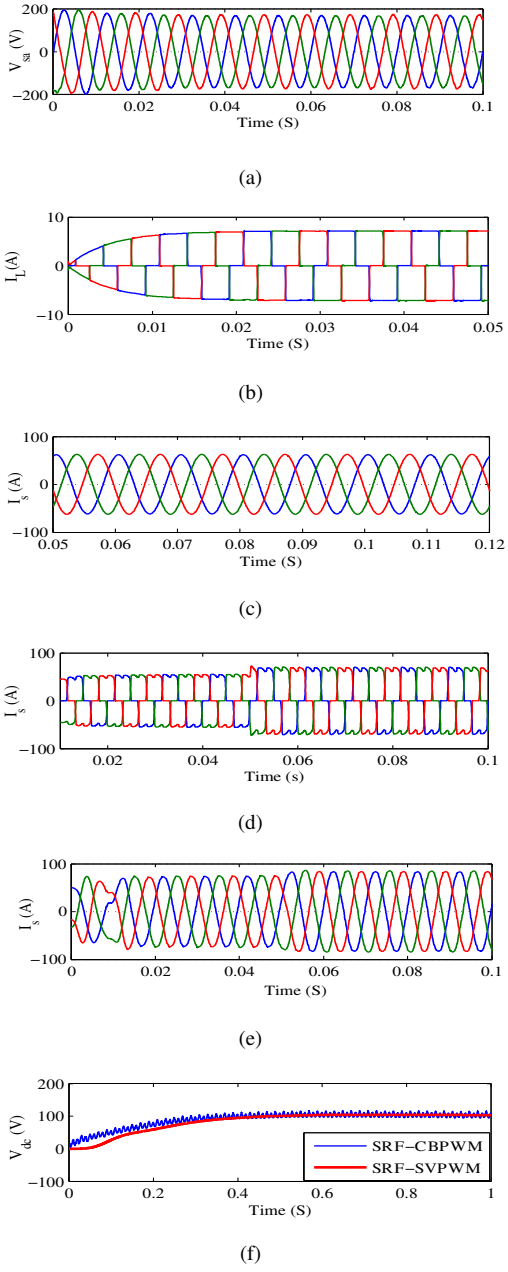

Fig. 5. (a) supply voltage, Steady state response of (b)Load current (c)source current, Transient response of(d)load current (e)source current for SRF-SVPWM based HSAPF(f) DC-link voltage for both SRF-CBPWM and SRF-SVPWM

SRF-CBPWM control technique) with both steady state and dynamic condition of load are given in Fig. 6. This paper proofs by MATLAB simulation that both control technique under ideal supply condition with steady state as well as dynamic condition of non-linear load and results works better, bringing down the THD of source current below 5% from the THD of source current of 37% before compensation. SRF-SVPWM based HSAPF yields better result in comparision to HSAPF with SRF-CBPWM. The THD of source current is decreased to 2.27% for SRF-CBPWM and 1.27% for SRF-

TABLE I
DATA TABLE

Line voltage and Frequency	$V_s = 220V(RMS), f_s = 50Hz$
Line impedance	$L_s = 0.5mH, R_s = 0.1\Omega$
Current source type of non linear load impedance	$L_L = 20mH, R_L = 50\Omega$
Series active filter parameter Shunt passive filter parameter	$C_c = 60\mu F, L_c = 1.35mH, C_{dc} = 2000\mu F, V_{dc} = 120V$ $L_f = 1.86mH, C_f = 60\mu F$

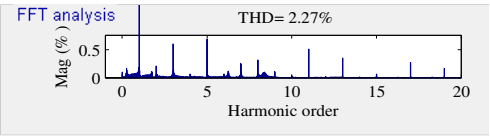

(a)

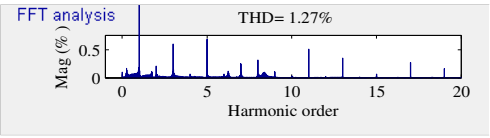

(b)

Fig. 6. (a) THD of source current for SRF-CBPWM(b)THD of source current for SRF-SVPWM

SVPWM from the THD of source current of 37% before compensation.

VII. CONCLUSIONS

In this paper the design of controller of a 3-phase HSAPF is presented and analysed. Furthermore, SRF method is used as control algorithm for reference generation and SVPWM helps in the generation of modulated signal. This paper scrutinizes the correlation between SRF-SVPWM and SRF-CBPWM. Characteristically SRF-SVPWM uses carrier for switching pattern generation but there is a dissimilarity in between them is that the switching pattern of SVPWM are obtained by vector calculation and the switching signal of CBPWM is sine wave or sine wave with common mode injection. Thus the switching signal of SVPWM has fascilitates switchings that decreases the distortion in output voltage waveform. SVPWM fully utilizes dc-link voltage for switching pattern generation but it can not be utilised properly by CBPWM. This paper verified by computer simulation that the performance of SRF-SVPWM based HSAPF is superior than HSAPF with SRF-CBPWM. Also the THD of SRF-SVPWM based HSAPF is less in comparision to HSAPF with SRF-CBPWM.

REFERENCES

[1] D. Rivas, L. Moran, J. W. Dixon, and J. R. Espinoza, "Improving passive filter compensation performance with active techniques," Industrial Electronics, IEEE Transactions on, vol. 50, no. 1, pp. 161–170, 2003.

[2] H.-L. Jou, J.-C. Wu, and K.-D. Wu, "Parallel operation of passive power filter and hybrid power filter for harmonic suppression," in Generation, Transmission and Distribution, IEE Proceedings-, vol. 148, pp. 8–14, IET, 2001.

[3] A. Sharaf, H. Huang, and L. Chang, "Power quality and nonlinear load voltage stabilization using error-driven switched passive power filter," in Industrial Electronics, 1995. ISIE'95., Proceedings of the IEEE International Symposium on, vol. 2, pp. 616–621, IEEE, 1995.

[4] H. Akagi, "Trends in active power line conditioners," Power Electronics, IEEE Transactions on, vol. 9, no. 3, pp. 263–268, 1994.

[5] L. Asiminoaei, E. Aeloiza, P. N. Enjeti, and F. Blaabjerg, "Shunt active-power-filter topology based on parallel interleaved inverters," Industrial Electronics, IEEE Transactions on, vol. 55, no. 3, pp. 1175–1189, 2008.

[6] H. Akagi, "Active harmonic filters," Proceedings of the IEEE, vol. 93, no. 12, pp. 2128–2141, 2005.

[7] M. Benhabib and S. Saadate, "New control approach for four-wire active power filter based on the use of synchronous reference frame," Electric Power Systems Research, vol. 73, no. 3, pp. 353–362, 2005.

[8] S. Rahmani, K. Al-Haddad, and F. Fnaiech, "A new control technique based on the instantaneous active current applied to shunt hybrid power filters," in Power Electronics Specialist Conference, 2003. PESC'03. 2003 IEEE 34th Annual, vol. 2, pp. 808–813, IEEE, 2003.

[9] J. Liu, J. Yang, and Z. Wang, "A new approach for single-phase harmonic current detecting and its application in a hybrid active power filter," in Industrial Electronics Society, 1999. IECON'99 Proceedings. The 25th Annual Conference of the IEEE, vol. 2, pp. 849–854, IEEE, 1999.

[10] M. Aredes and E. H. Watanabe, "New control algorithms for series and shunt three-phase four-wire active power filters," Power Delivery, IEEE Transactions on, vol. 10, no. 3, pp. 1649–1656, 1995.

[11] M. M. A. Radzi and N. A. Rahim, "Neural network and bandless hysteresis approach to control switched capacitor active power filter for reduction of harmonics," Industrial Electronics, IEEE Transactions on, vol. 56, no. 5, pp. 1477–1484, 2009.

[12] J.-f. Jiang, H.-j. Liu, Y.-p. Chen, and J.-j. SUN, "A novel double hysteresis current control method for active power filter with voltage space vector," PROCEEDINGS-CHINESE SOCIETY OF ELECTRICAL ENGINEERING, vol. 24, no. 10, pp. 82–86, 2004.

[13] B. Singh, K. Al-Haddad, and A. Chandra, "Active power filter with sliding mode control," IEE Proceedings-Generation, Transmission and Distribution, vol. 144, no. 6, pp. 564–568, 1997.

[14] X. Hao, X. Yang, T. Liu, L. Huang, and W. Chen, "A sliding-mode controller with multiresonant sliding surface for single-phase grid-connected vsi with an lcl filter," Power Electronics, IEEE Transactions on, vol. 28, no. 5, pp. 2259–2268, 2013.

[15] Y. Tang, P. C. Loh, P. Wang, F. H. Choo, F. Gao, and F. Blaabjerg, "Generalized design of high performance shunt active power filter with output lcl filter," Industrial Electronics, IEEE Transactions on, vol. 59, no. 3, pp. 1443–1452, 2012.

[16] O. Vodyakho and C. C. Mi, "Three-level inverter-based shunt active power filter in three-phase three-wire and four-wire systems," Power Electronics, IEEE Transactions on, vol. 24, no. 5, pp. 1350–1363, 2009.

[17] T. Ya-fei, H. Ji-ai, and Z.-w. HUANG, "Simulation and analyzation of space vector pwm [j]," Proceedings of Electric Power System and Automation, vol. 4, 2004.